PNAS
www.pnas.org

Supplementary Information for

Insect biomass decline scaled to species diversity: general patterns derived from a hoverfly community

Caspar A. Hallmann, Axel Ssymank, Martin Sorg, Hans de Kroon, Eelke Jongejans

Corresponding Author name.
E-mail: c.hallmann@science.ru.nl

This PDF file includes:

Supporting Information Text

Supplementary Methods.

Determining the relative biomass contribution of Hoverflies. In order to assess how much hoverflies contribute to the total biomass (of all flying insects) in the malaise traps, we utilized two independent datasets. We used measurements of body length made by the Krefeld Entomological Society (Axel Ssymank, all species in our data), and fresh-weight measurements kindly provided by Nick Hofland (Radboud University). The fresh-weight data were collected in 2016 and 2017 and included in total 97 measurements, over 13 hoverfly genera). We then paired the two datasets by species (if unknown, by genus) and regressed the log of the body weight to body length (intercept = -6.33, slope coefficient= 0.24). The resulting model coefficients were used to allometrically predict the weight per individual in our data, which were subsequently summed over all individuals per year. Based on these calculations, we predicted total hoverfly mass of 321.6 and 52.2 gram for 1989 and 2014, respectively. This implied a relative contribution of 4.4% and 3.0% to the total flying insect biomass collected in the Wahnbachtal malaise traps in 1989 and 2014, respectively.

Steps in deriving hypothetical scenarios of variation species decline rate. In the main text, we describe three alternative hypothetical scenarios of species decline rates. Here we describe the steps and assumptions that were made while designing these scenarios. We started off with a rank-abundance curve that was similar to the observed rank-abundance curve of the hoverflies (Fig. 2B in the main text), i.e. by using a zipf-mandelbrot distribution with arbitrary parameters of $\beta_0 = -1.5$ and $beta_1 = 2$ (see equation 4 in main text), for a pool of 200 species. The total hoverfly community was scaled so that the most abundant species arbitrarily consisted of 1500 individuals. Next we defined the rate of decline in each of the three scenarios. For equal rates of decline between species (scenario I) we set $\lambda_i = 0.2$, i.e. at 80% decline for each species i. In scenarios II and III we allowed decline rates to scale linearly to species rank, where the relationship was negative in scenario II and positive in scenario III, at arbitrary slopes of -0.015 and 0.020, respectively. Finally we scaled the resulting species decline rate vector in order to achieve a total abundance loss of 80% (see Fig. 1A in main text). Using these three scenarios of hypothetical decline rates, we proceeded in calculating persistence (equation 1), rank abundance distributions, and fraction of species lost (Fig. 1B,C,D), under perfect and imperfect (at 40%) detection efficiency. We also examined how other diversity measures, i.e. Hill numbers (1, 2) of orders 0, 1, 2, and 3, behave in the presence of the three scenarios of decline rates, and under imperfect detection. To this end, we simulated 1000 hypothetical hoverfly communities (based on parameters as above) and for each community we calculated the percentage change in Hill numbers of orders q=0-3 (see Fig. S1).

Approximating average seasonal species availability. If detectability of individual species is invariant during the season, i.e. they are equally likely to be trapped on each of the sampling days, then the distribution of number of species in each pot could be approximated in a straightforward manner by a sampling-without-replacement process, conditional on the accumulated community data. However, hoverfly species are not likely to be active during the entire season, leading to non-uniform detectability during the season. Formally, the number of species expected to be trapped in a single pot ($\hat{s}$) will depend on the relative abundance of each species (N_i), the total abundance in the pot (N_j) and total species richness S, according to

$$\hat{s}(N_j, S) = \sum_{i}^{S} \left(1 - \frac{\binom{N-N_i}{N_j}}{\binom{N}{N_j}} \right)$$

(3) where $N = \sum N_j = \sum N_i$.

In equation 11, main text, we introduced a correction factor c, that measures the average availability of species during the season. We used the following approach to obtain an estimate of c.

First we produced average daily total abundance per pot j (abundance per pot divided by exposure length) which we denote as $\hat{n}_j$. We then calculated the expected number of species given total richness (S), total abundance (N) and relative species abundance (N_i). Additionally, and for each pot, we calculated the expected number of species per day conditional on the number of species seen in each pot (S_j).

$$\hat{s}_j^{(2)}(\hat{n}_j, S_j) = \sum_{i}^{S_j} \left(1 - \frac{\binom{N-N_i}{\hat{n}_j}}{\binom{N}{\hat{n}_j}} \right)$$

The relationship between $\hat{s}_j^{(1)}(\hat{n}_j, S)$ and $\hat{s}_j^{(2)}(\hat{n}_j, S_j)$ is linear, with zero intercept and slope $0 < c \leq 1$, because typically $S_j \leq S$. The coefficient c is hence obtained as:

$$c = \frac{\hat{s}_j^{(2)}(\hat{n}_j, S_j)}{\hat{s}_j^{(2)}(\hat{n}_j, S)}$$

.

Supplementary Figures

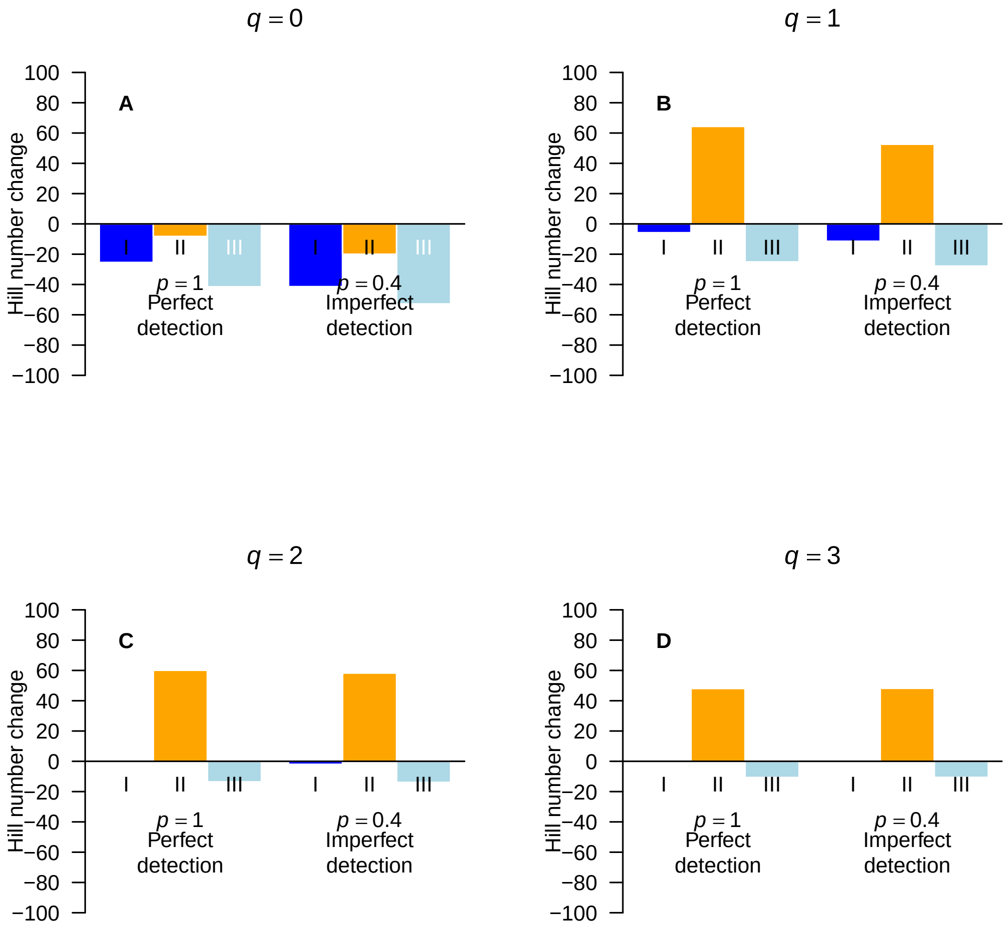

Fig. S1. Change in diversity measures (Hill numbers for orders $q \in \{0, 1, 2, 3\}$) in each theoretical scenario under perfect (p=100%) and imperfect (p=40%) sampling efficiency. A: Change in species richness (q=0), B: Change in Shannon diversity (q=1), C: Change in inverse Simpson index (q=2), D: Change in a higher-order diversity measure (q=3).

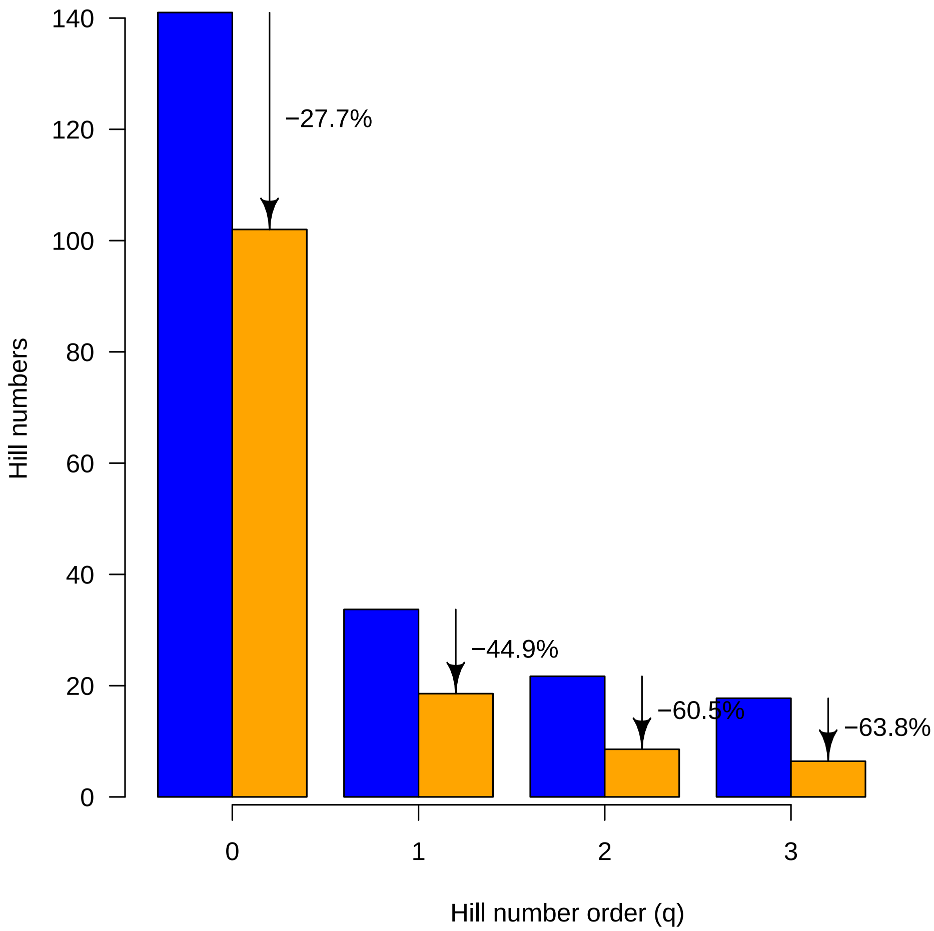

Fig. S2. Hill numbers of order 0-3 for 1989 (blue bars) and 2014 (orange bars), with accompanying amount of decline between the years. Orders of 0-2 denote species richness, exponent of Shannon entropy, and Simpson diversity, respectively, while for q=3 emphasis is placed predominantly on the more common species in the assemblages.

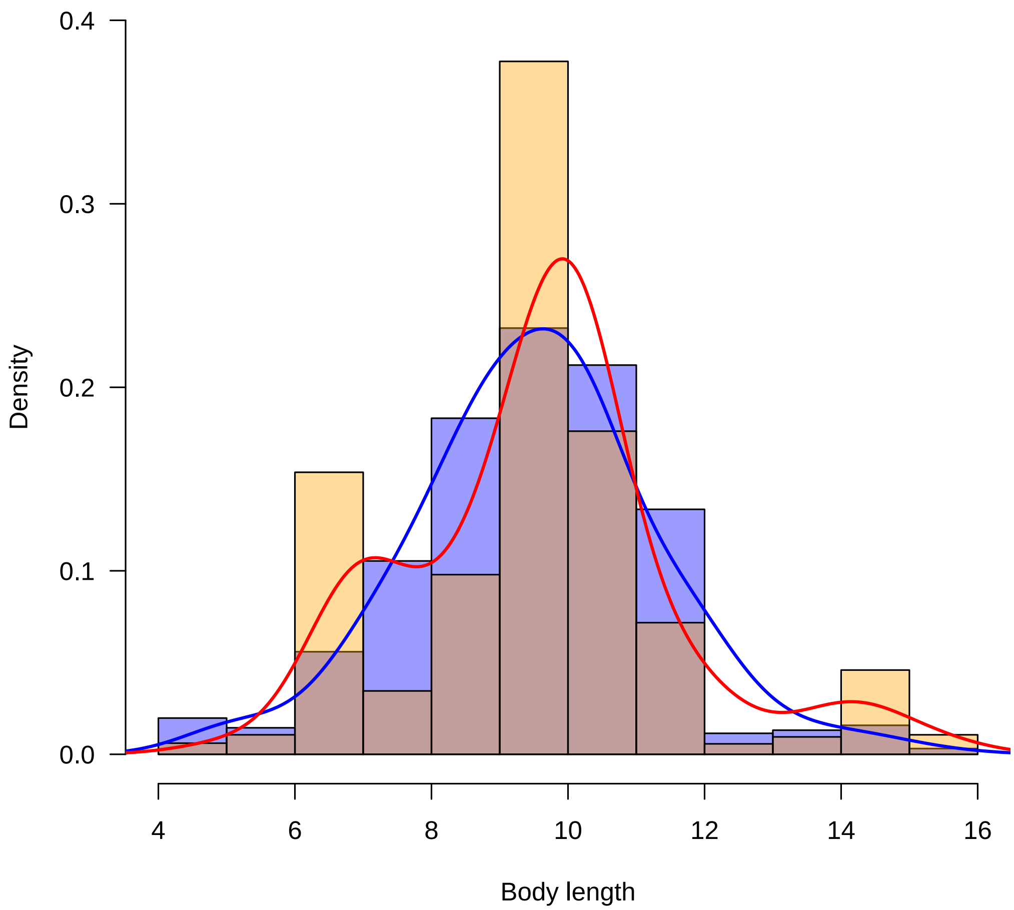

Fig. S3. Distribution of body length weighted by specie's abundances for 1989 (blue) and 2014 (red)

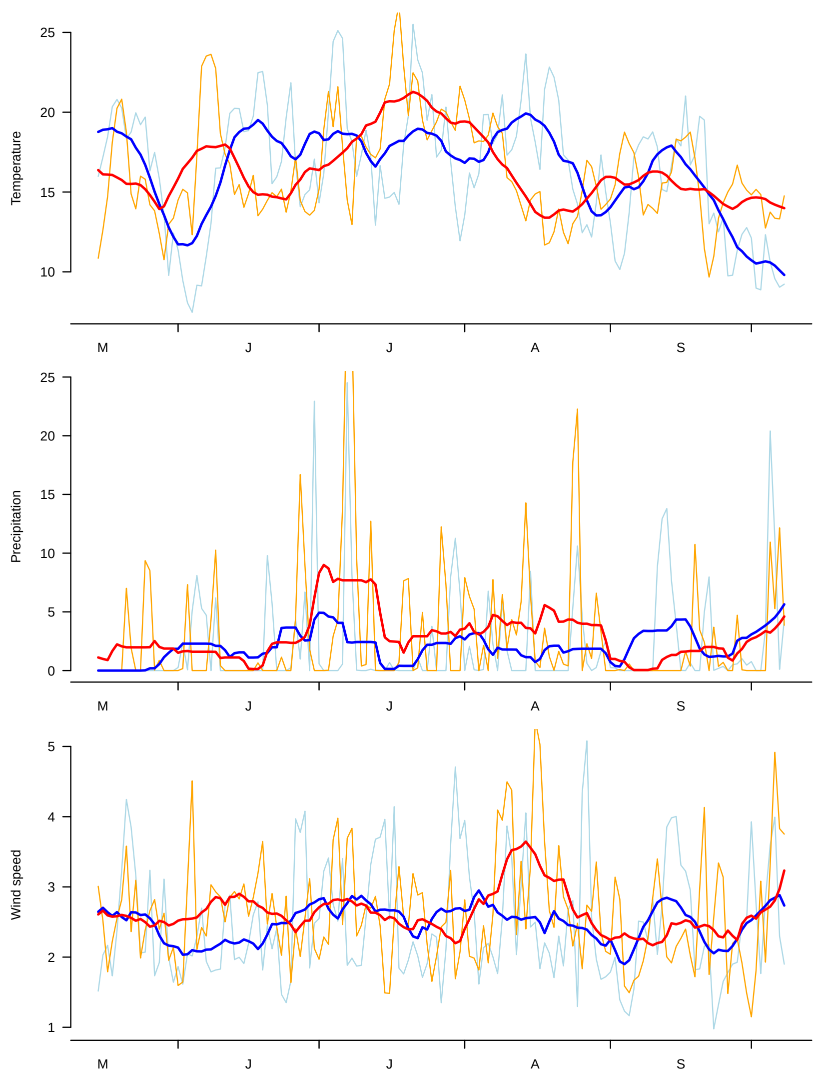

Fig. S4. Climatic variables in 1989 (light blue) and 2014 (orange) for temperature (in C^o), precipitation (mm/day) and wind speed (m/s). Thick red and blue lines represent the 2-week moving average.

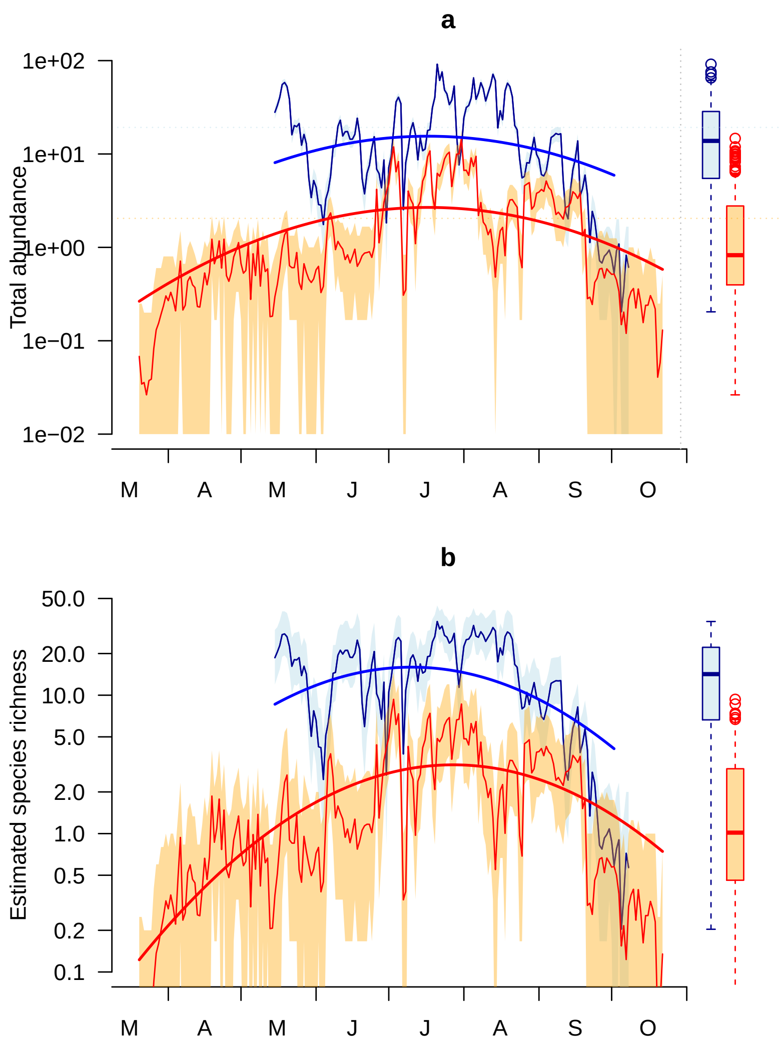

Fig. S5. Seasonal trajectory of estimated number of hoverfly individuals (A) and species (B) in 1989 (blue) and 2014 (red) along with 95% credible intervals. Boxplots provide the distribution of the mean daily values over the two seasons.

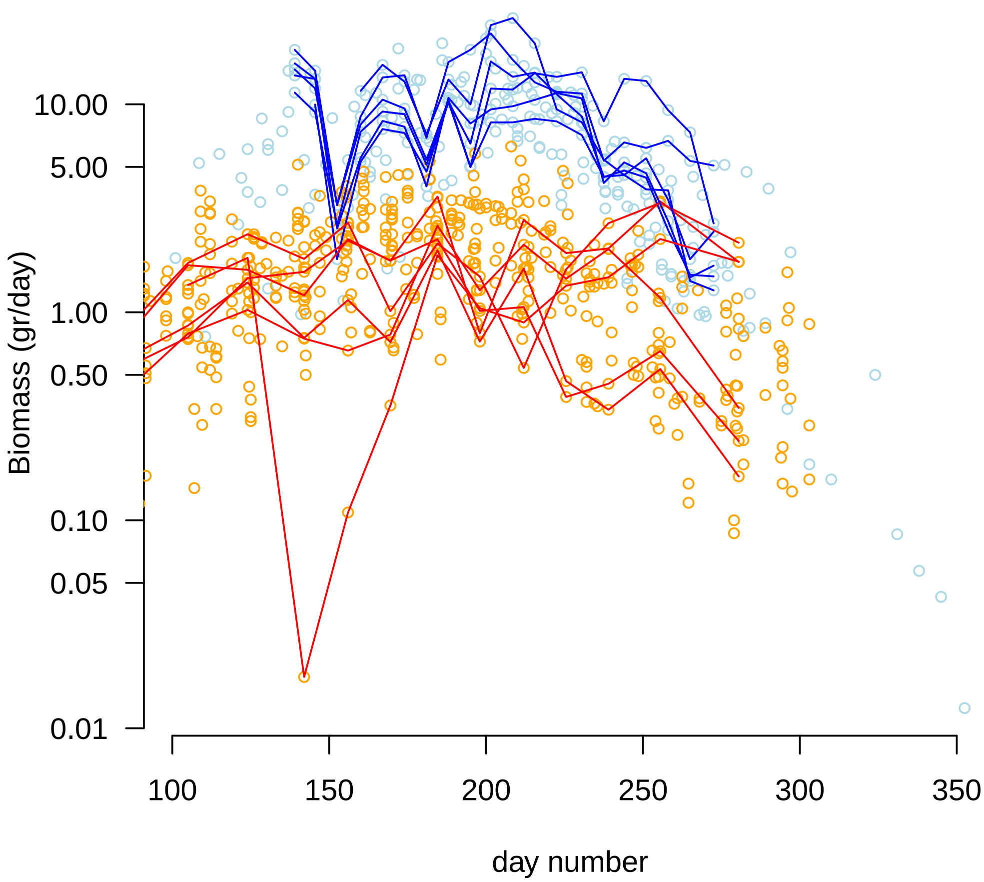

Fig. S6. Temporal distribution of biomass (in gram per day) of total flying insects for all pots in the period 1989-1992 (light blue dots) and period 2012-2015 (orange dots). Blue and red lines depict the seasonal biomass distribution for the six Wahnbachtal traps examined in 1989 and 2014

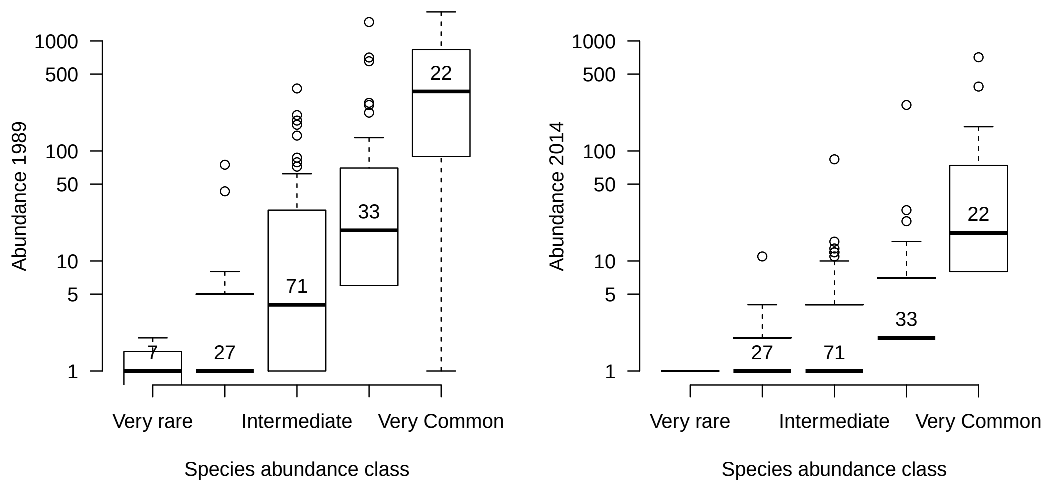

Fig. S7. Observed abundance (sum of 1998 and 2014 by species) versus abundance-class of species in Germany as classified in (4). Numbers inside boxplots represent the number of species in that class

Supplementary Tables

Table S1. Parameter estimates from posterior distribution for daily total hoverfly abundance. d: climatic parameters. c: seasonal (quadratic effect) parameters, b: trap effects, and log(λ): the log-rate of decline from 1989 to 2014.

	mean	sd	2.5%	97.5%	$\hat{R}$
Intercept	2.477	0.027	2.424	2.529	1.002
log(λ)	-1.756	0.028	-1.808	-1.697	1.001
c_1	0.090	0.014	0.063	0.116	1.001
c_2	-0.480	0.019	-0.516	-0.443	1.002
c_3	0.476	0.033	0.412	0.541	1.001
c_4	-0.614	0.035	-0.683	-0.548	1.001
d_1	0.590	0.013	0.564	0.615	1.001
d_2	-0.367	0.032	-0.432	-0.310	1.001
d_3	-0.048	0.023	-0.094	-0.003	1.001
b_2	0.318	0.027	0.264	0.371	1.001
b_3	0.024	0.028	-0.031	0.082	1.002
b_4	0.631	0.025	0.583	0.678	1.001
b_5	0.629	0.025	0.581	0.678	1.001
b_6	-0.050	0.029	-0.107	0.007	1.001

Table S2. Parameter estimates from posterior distribution for daily hoverfly species richness. d: climatic parameters. c: seasonal (quadratic effect) parameters, b: trap effects, and log(λ): the log-rate of decline from 1989 to 2014.

	mean	sd	2.5%	97.5%	$\hat{R}$
Intercept	2.748	0.048	2.656	2.846	1.002
log(λ)	-1.671	0.040	-1.750	-1.592	1.001
c_1	-0.036	0.033	-0.101	0.029	1.002
c_2	-0.571	0.041	-0.652	-0.491	1.002
c_3	0.325	0.024	0.277	0.373	1.001
c_4	-0.568	0.029	-0.627	-0.514	1.001
d_1	0.349	0.019	0.311	0.385	1.003
d_2	-0.271	0.030	-0.331	-0.212	1.002
d_3	-0.010	0.023	-0.054	0.035	1.001
b_2	0.031	0.054	-0.076	0.139	1.002
b_3	-0.112	0.053	-0.217	-0.009	1.004
b_4	0.185	0.051	0.081	0.281	1.001
b_5	0.117	0.051	0.019	0.215	1.003
b_6	-0.100	0.059	-0.215	0.016	1.003

References

1. Hill MO (1973) Diversity and evenness: a unifying notation and its consequences. *Ecology* 54(2):427–432.
2. Chao A, et al. (2014) Rarefaction and extrapolation with hill numbers: a framework for sampling and estimation in species diversity studies. *Ecological Monographs* 84(1):45–67.
3. Oksanen J, et al. (2018) *vegan: Community Ecology Package.* R package version 2.5-2.
4. Ssymank A, Doczkal D, Rennwald K, Dziock F (2011) Rote Liste und Gesamtartenliste der Schwebfliegen (Diptera: Syrphidae) Deutschlands. Rote Liste gefährdeter Tiere, Pflanzen und Pilze Deutschlands Band 3, Teil 1. *Naturschutz und Biologische Vielfalt* 70(3):13–83.